Hyperbolic chaos at blinking coupling of noisy oscillators

Pavel V. Kuptsov,[1,2,*] Sergey P. Kuznetsov,[2,3] and Arkady Pikovsky[2]

[1]*Department of Instrumentation Engineering, Saratov State Technical University, Politekhnicheskaya 77, Saratov 410054, Russia*

[2]*Institute of Physics and Astronomy, University of Potsdam, Karl-Liebknecht-Str. 24/25, 14476 Potsdam-Golm, Germany*

[3]*Kotel'nikov's Institute of Radio-Engineering and Electronics of RAS, Saratov Branch, Zelenaya 38, Saratov 410019, Russia*

We study an ensemble of identical noisy phase oscillators with a blinking mean-field coupling, where one-cluster and two-cluster synchronous states alternate. In the thermodynamic limit the population is described by a nonlinear Fokker-Planck equation. We show that the dynamics of the order parameters demonstrates hyperbolic chaos. The chaoticity manifests itself in phases of the complex mean field, which obey a strongly chaotic Bernoulli map. Hyperbolicity is confirmed by numerical tests based on the calculations of relevant invariant Lyapunov vectors and Lyapunov exponents. We show how the chaotic dynamics of the phases is slightly smeared by finite-size fluctuations.

　　　　　　PACS number(s): 05.45.Jn, 05.10.Gg, 89.75.Kd

I. INTRODUCTION

Dynamics of large populations of coupled oscillators attracted large interest recently. Problems of this type appear in studies of Josephson junctions, lasers, ensembles of neurons, cell populations, and many other fields. From a more general perspective, studies of such a system allow one to shed light on a long-standing problem of an interrelation between microscopic and macroscopic dynamics. Indeed, the mostly studied nontrivial effect in the ensembles of globally coupled oscillators is their synchronization, which can be considered as a nonequilibrium phase transition [1,2]. Remarkably, in some situations one can explicitly derive the dynamics of global variables (order parameters), in terms of which the synchronization transition is a bifurcation from a zero equilibrium to a nontrivial state [3].

Different interrelations between regularity properties on micro- and macro-levels (i.e., for the individual oscillators and for the mean fields) have been reported in the literature. For example, chaotic micro-oscillators being coupled may lead to periodic mean fields [4–8]. On the other hand, coupled periodic oscillators may produce chaotic mean fields [9–11]. While a general description of populations of deterministic oscillators remains a challenging task, there exists a nice framework for ensembles of noise-driven oscillators. The behavior in the thermodynamic limit can be described self-consistently by virtue of a nonlinear Fokker-Planck equation, first suggested by Desai and Zwanzig [12] in the context of globally coupled noisy bistable oscillators (see also Ref. [13]). This approach has been then applied to noisy periodic oscillators in Refs. [14,15].

In this paper, we consider a population of noisy oscillators subject to a blinking, time-periodic coupling [16–18]. This is a minimal generalization of the simplest model with a constant coupling, demonstrating simple synchronization patterns only. We will show that with a blinking coupling, where on different periods of the total cycle different synchronous modes emerge, the total dynamics demonstrates highly nontrivial regime of

phase hyperbolic chaos. In this regime, the phase of the complex order parameter obeys a doubling Bernoulli map, which has strong chaotic properties, and is, contrary to many other models of chaos, structurally stable in respect to perturbations.

Our treatment of the dynamics of the complex mean fields follows recent studies [19,20], where a general framework for mechanisms of hyperbolic chaos in coupled oscillators has been developed. In the simplest setup, two oscillators that are excited alternately can interact in a way to influence the phases of each others at the stages where these oscillators pass through a supercritical Hopf bifurcation. More precisely, one needs the appearing field to be forced by a higher harmonic of another oscillator, then a transformation of the phase $\phi \to n\phi$ with $|n| \geqslant 2$ can occur. As a result, the phase obeys a Bernoulli-type, uniformly expanding map, and the whole strange attractor is of a famous Smale-Williams type [21]. The described mechanism of hyperbolic chaos generation via the phase multiplication is quite generic. The straightforward way of its implementation is to consider two nonautonomous limit-cycle oscillators with different natural frequencies and appropriate coupling [22]. Further analysis revealed a possibility to identify this mechanism in a system of two or three coupled autonomous oscillators [23]. Recently, it has been described how to observe the hyperbolic chaos in a spatially extended system, as a result of an interaction of Turing modes [24]. In Ref. [11] an alternation between synchronized and desynchronized regimes in two ensembles of nonidentical oscillators subjected to the Kuramoto transition was shown to possess a collective hyperbolic chaos of complex order parameters.

In this paper, we report on our study of an ensemble of identical stochastic phase oscillators coupled via the mean fields. We consider a situation of blinking coupling, where different synchronization patterns, one with one cluster and another with two clusters, alternate. We show, both basing on the nonlinear Fokker-Planck equation and on the direct simulation of a large population, that the phases of these patterns demonstrate hyperbolic chaos. Moreover, we study the Lyapunov exponents of the system and apply numerical criteria based on Lyapunov vectors to verify hyperbolicity.

---

*p.kuptsov@rambler.ru

II. ENSEMBLE OF COUPLED NOISY OSCILLATORS

A. Microscopic equations

Our basic model is an ensemble of K globally coupled identical limit-cycle oscillators with additive noise. In the phase description, the ensemble is governed by the following set of equations:

$$\dot{\phi}_k = f(\phi_k) + \frac{1}{K}\sum_{j=1}^{K} q(\phi_j - \phi_k) + \sigma \xi_k(t), \qquad (1)$$

where $k = 1, \ldots, K$, ϕ_k is the phase of a kth oscillator (taken in the reference frame rotating with the basic frequency), and the independent random variables $\xi_k(t)$ describe white Gaussian noise: $\langle \xi_k(t)\xi_j(t + \tau)\rangle = \delta_{jk}\delta(\tau)$. Functions $q(\phi)$ and $f(\phi)$ (both are 2π-periodic) describe, respectively, effects of global coupling and of the external periodic forcing at the oscillator frequency and/or its harmonics. It is convenient to define these functions by means of the Fourier decompositions:

$$f(\phi) = \sum_{n=-\infty}^{\infty} F_n e^{in\phi}, \quad q(\phi) = \sum_{n=-\infty}^{\infty} Q_n e^{in\phi}. \qquad (2)$$

Since the functions f and q are real, $F_{-n} = F_n^*$, and $Q_{-n} = Q_n^*$, where asterisk denotes complex conjugation.

Given a state of the ensemble, one can determine the following mean fields playing roles of order parameters:

$$A_\ell(t) = \langle e^{i\ell\phi}\rangle = \frac{1}{K}\sum_{k=1}^{K} e^{i\ell\phi_k}, \qquad (3)$$

where $\ell = 1, 2, \ldots$, and $A_0 = 1$. Notice that $A_{-\ell} = A_\ell^*$. In what follows we shall use the notation $\arg A_\ell = \Phi_\ell$.

B. Nonlinear Fokker-Plank equation

In the thermodynamic limit $K \to \infty$, the ensemble can be described by the density of the probability distribution $v(\phi,t)$. The mean fields in this case are expressed as

$$A_\ell(t) = \int_0^{2\pi} v(\phi,t)e^{i\ell\phi}d\phi. \qquad (4)$$

The probability density can be decomposed as Fourier series:

$$v(\phi,t) = \frac{1}{2\pi}\sum_{\ell=-\infty}^{\infty} A_\ell(t)e^{-i\ell\phi}, \qquad (5)$$

i.e., the order parameters $A_\ell(t)$ are just the coefficients of the Fourier modes for the probability density.

The dynamics of the probability density can be described by the nonlinear Fokker-Planck equation [12,13]. For the system Eq. (1), accounting for the expressions in Eq. (2), we can write:

$$\frac{\partial v}{\partial t} = -\frac{\partial}{\partial \phi}\sum_{n=-\infty}^{\infty} v(F_{-n} + Q_n A_n)e^{-in\phi} + \frac{\sigma^2}{2}\frac{\partial^2 v}{\partial \phi^2}. \qquad (6)$$

Now we substitute here the Fourier decomposition Eq. (5) for $v(\phi,t)$, then multiply the expression by $e^{-i\ell\phi}$, and integrate it over 2π. The resulting equations for A_ℓ read:

$$\dot{A}_\ell = i\ell \sum_{n=-\infty}^{\infty} (F_{-n} + Q_n A_n)A_{\ell-n} - \frac{\sigma^2\ell^2}{2}A_\ell. \qquad (7)$$

C. Elementary synchronization dynamics

The set of Eqs. (7) allows one a simple qualitative description of basic synchronization phenomena in the ensemble. If only the global coupling is present ($F_n = 0$), and $q(\phi)$ has one Fourier component $Q_n = -\frac{i}{2}\kappa_n$, then the nonsynchronized state $A_j = \delta_{j,0}$ remains stable until the coupling exceeds the synchronization threshold

$$\kappa_n > n\sigma^2. \qquad (8)$$

Above this threshold, the mode A_n becomes unstable, and a stationary solution of Eq. (7) containing modes $A_{\ell n}$ with $\ell = 1,2,3,\ldots$ is established. This corresponds to the appearance of an n-clustered state of the ensemble, where the probability density has maxima at $\phi^{(0)} + k2\pi/n$, and $\phi^{(0)}$ is an arbitrary phase shift determined by initial conditions. In contrast, without the global coupling ($Q_n = 0$), if only the external forcing is present containing one Fourier component ($F_n = -\frac{i}{2}\epsilon$), then for a small ϵ an n-cluster state with $A_n \approx -\epsilon n^{-1}\sigma^{-2}$ appears. The phase of this cluster is fixed, determined by the applied forcing.

III. CLUSTER EXCHANGE DYNAMICS AT BLINKING COUPLING

The main goal of this paper is to describe macroscopic chaos appearing when the coupling in the ensemble is blinking (cf. Ref. [16]).

In this section, we consider the effect of blinking coupling qualitatively, based on the elementary synchronization dynamics described in the previous section. First, we make a particular choice for the global coupling terms, assuming alternating couplings Q_1 and Q_2:

$$Q_{1,2} = -\frac{i\tilde{\kappa}_{1,2}(t)}{2}, \qquad (9)$$

where

$$(\tilde{\kappa}_1, \tilde{\kappa}_2) = \begin{cases} (\kappa_1, 0), & \text{if } mT \leqslant t < mT + T/2, \\ (0, \kappa_2), & \text{if } mT + T/2 \leqslant t < mT + T. \end{cases} \qquad (10)$$

Here, T is the total period of blinking; it is assumed to be large enough compared to the characteristic time of cluster formation or decay. In the first half of this period (we call it stage 1) only Q_1 is present; correspondingly, the one-cluster state develops. During the second half of the period (stage 2), only Q_2 is present; so, in this stage, the two-cluster state develops (see Fig. 1 below).

For the following consideration, the phases of the clusters are important. As the one-cluster state contains all modes A_n, $n = 1,2,3,\ldots$, at the beginning of stage 2 the amplitude $A_2 \sim A_1^2$ is finite. During stage 2, due to the appropriate coupling, the instability appears associated with formation of the two-cluster state, and the initial phase $\Phi_2 = 2\Phi_1$ occurs, to be definite, determined by the preceding evolution. Thus, the two-cluster state accepts this phase from the former one-cluster state. At the end of stage 2, only modes with even index A_n, $n = 2,4,6,\ldots$ are present (as T is large enough, the odd modes decay effectively during stage 2). Thus, at the beginning of the next stage 1, there is no initial amplitude A_1, and its growth due to the coupling Q_1 would start only from random initial
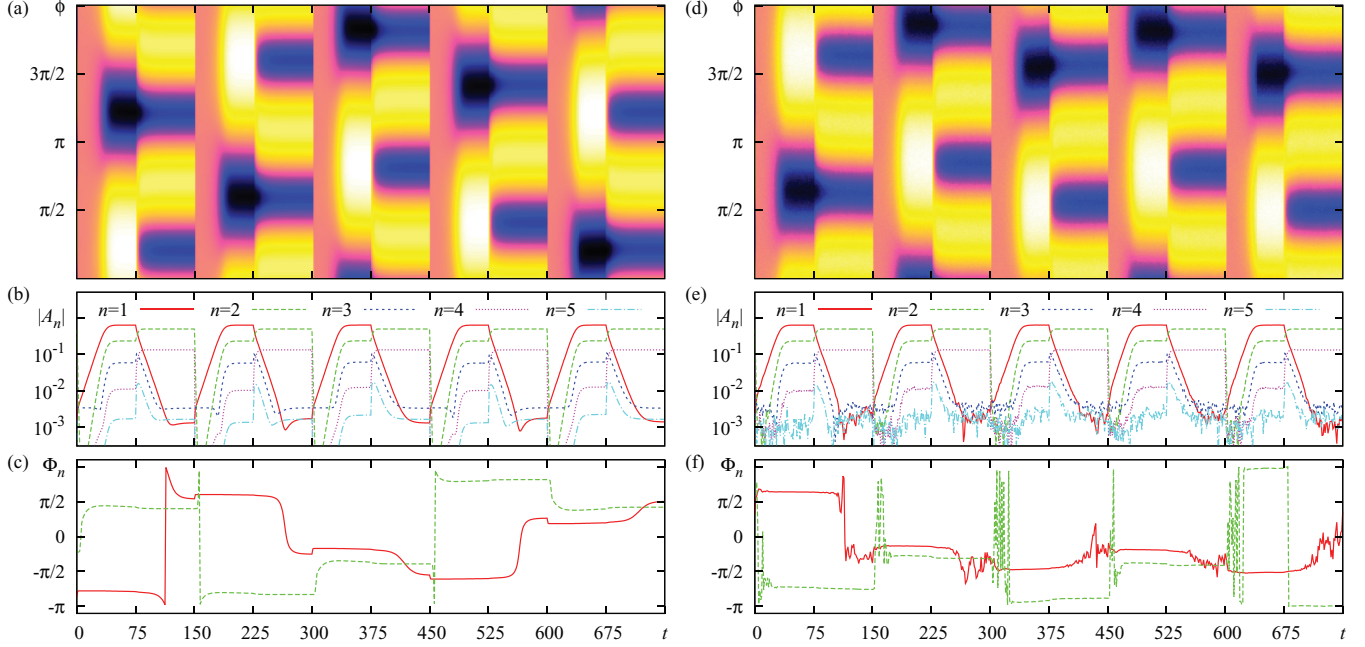
FIG. 1. (Color online) (a) Probability density $v(\phi,t)$ determined by Eq. (5), where $A_n(t)$ are computed according to Eq. (12); (d) distribution for the ensemble of ϕ_k [see Eq. (14)], where the total number of the oscillators is $K = 10^6$. Darker colors correspond to higher values of $v(\phi,t)$. Five periods of switching of $\tilde{\kappa}_{1,2}(t)$ are shown. (b) and (c) Absolute values and arguments of A_n computed according to Eq. (12); (e) and (f) are the same computed via Eq. (3) for the ensemble. $|A_n|$ are plotted in logarithmic scale. Parameters: $\kappa_1 = 1.3$, $\kappa_2 = 2.3$, $T = 150$, $\epsilon = 0.01$, $\sigma = 1$, $\ell_{\text{cut}} = 10$.

fluctuations, and the appearing one-cluster state would have a random phase.

The situation changes if a small regular external forcing is present. As one can see from Eq. (7), the forcing F_n provides appearance of terms $\sim i F_{-n} A_{\ell-n}$, thus producing combinational modes.

Let us consider the effect of the mode $F_3 = -\frac{i\epsilon}{2}$. At stage 1, it produces combinational modes with all indices, but because these modes are already present in the distribution, the effect of small ϵ is negligible. At stage 2, however, the mode A_1 is produced by terms $F_3^* A_2^* + F_3 A_4$ in Eq. (7). Because A_2 is typically much larger than A_4, the result of this interaction is the appearance of a small but notable amount of mode 1 with $A_1 \sim \epsilon A_2^*$ at the end of stage 2.

This circumstance changes, essentially, the starting conditions for the evolution on stage 1 compared to the case $\epsilon = 0$: now the growing mode A_1 develops from the seed $\sim\epsilon A_2^*$, and so its phase will be $\Phi_1 = -\Phi_2$. Now the phases of cluster states arising at all stages of evolution are nonrandom but depend on the previous phases in a deterministic way. Combining the transformations $\Phi_2 = 2\Phi_1$ at the transition from stage 1 to stage 2, and $\Phi_1 = -\Phi_2$ at the transition from stage 2 to stage 1, we obtain the Bernoulli-type map

$$\Phi_1(m + 1) = -2\Phi_1(m) \qquad (11)$$

at successive periods of the blinking coupling.

The map [Eq. (11)] for the phase transformation is uniformly expanding and hyperbolic, and we conclude from these qualitative arguments that the cluster patterns for the blinking coupling of noisy oscillators in the situation we have considered will demonstrate hyperbolic chaos in the

dynamics of the order parameters (the modes of the distribution density).

IV. ILLUSTRATIONS AND CHARACTERIZATION OF THE DYNAMICS

In this section we confirm numerically the existence of the hyperbolic chaos in the setup described above. The mode equations take the form

$$\dot{A}_\ell = \frac{\ell}{2} \left[\sum_{n=1}^{2} \tilde{\kappa}_n \left(A_n A_{\ell-n} - A_{-n} A_{\ell+n} \right) \right. $$
$$\left. + \epsilon(A_{\ell+3} - A_{\ell-3}) \right] - \frac{\sigma^2 \ell^2}{2} A_\ell. \qquad (12)$$

The corresponding Fokker-Plank equation reads

$$\frac{\partial v}{\partial t} = -\frac{\partial}{\partial \phi} \left\{ v \sum_{n=1}^{2} \tilde{\kappa}_n \left\langle \sin[n(\psi - \phi)] \right\rangle_\psi \right. $$
$$\left. + \epsilon v \sin 3\phi \right\} + \frac{\sigma^2}{2} \frac{\partial^2 v}{\partial \phi^2}, \qquad (13)$$

where $\langle \sin[n(\psi - \phi)] \rangle_\psi = \int_0^{2\pi} v(\psi,t) \sin[n(\psi - \phi)] d\psi$. Accounting this form, we can reconstruct the respective microscopic Eq. (1) for the ensemble of phase oscillators as

$$\dot{\phi}_k = \epsilon \sin(3\phi_k) + \sum_{n=1}^{2} \frac{\tilde{\kappa}_n}{K} \sum_{j=1}^{K} \sin[n(\phi_j - \phi_k)] + \sigma \xi_k(t).$$

$$(14)$$

In all these equations the blinking coupling $\tilde{\kappa}_n(t)$ is given by Eq. (10).

The essential control parameters both for the ensemble Eq. (14), and for the Fokker-Plank system Eq. (12) are κ_1 and κ_2, which have to satisfy the condition Eq. (8) for clusters to grow at the corresponding stages.

A. Nonlinear Fokker-Plank equation

First, we present numerics for the Fokker-Plank system Eq. (12). Since this system appears as a spectral decomposition of the nonlinear integrodifferential Eq. (13), it is stiff, and we integrate it numerically using the method of exponential time differencing; see Ref. [25]. As follows from Eq. (3), $|A_\ell| \leqslant 1$. Due to the terms proportional to ℓ^{-2}, the amplitudes of A_ℓ decay fast with ℓ. Direct verification shows that already for $\ell = 5$ the magnitude is small enough, $|A_5| \ll 1$, but to assure the validity of the numerical results we cut the infinite set of Eqs. (12) at $\ell_{\mathrm{cut}} = 10$.

Figure 1(a) illustrates the temporal behavior of the probability density $v(\phi,t)$ computed according to Eq. (5). At stage 1 $(0 \leqslant t \leqslant 75)$ the 1-cluster develops. Then, after the switch to stage 2 at $t = T/2 = 75$, the density acquires two humps. One part of the 2-cluster is located just at the site of the former 1-cluster, and the second one appears shifted by π. As we already discussed, this situation corresponds to the quadratic relation for the complex amplitudes $A_2 \sim A_1^2$ and to the doubling of the argument. At the initial epoch of the next stage 1 at $t \gtrsim 150$, the 2-cluster disappears, and the 1-cluster reappears. Notice that the hump emerges now at a site that is different both from that of the previous 2-cluster and that of the former 1-cluster. It is so because of the presence of a small force $f(\phi)$ corresponding to the term proportional to ϵ in Eqs. (12).

Figures 1(b) and 1(c) show magnitudes and arguments of A_n. At stage 1, all the magnitudes $|A_n|$ grow and saturate at some level; in this state, the main mode A_1 dominates. At stage 2, the mode A_2 grows, together with its harmonics, while all odd modes decay.

Let us now focus on the phase dynamics. The phase Φ_2 does not change at the transition from stage 1 to stage 2 at $t = 75$. At the beginning of stage 2, the phase of the first mode Φ_1 is nearly constant while the amplitude of this mode remains relatively large; however, at $t \approx 100$ the amplitude drops to the level $\sim \epsilon$, and now this mode is driven by ϵA_2^*. Here, the mode A_1 accepts the phase $-\Phi_2$ that can be seen in Fig. 1(c) as a sharp transition around $t \approx 110$. After this event, the phase of the mode A_1 does not vary significantly. At $t = T = 150$, the new stage 1 starts; here the amplitude of the previously active mode A_2 decays rapidly, but it reappears soon as the second harmonics of the mode 1, accepting its doubled phase $2\Phi_1$ (see the jump of Φ_2 at $t \approx 155$ followed by the growth of $|A_2|$).

Although the dynamics of the phases and the amplitudes observed in Figs. 1(a)–1(c) nicely correspond to the qualitative picture of Sec. II C, it is important to verify that the phase evolution really follows the Bernoulli-like map Eq. (11). In Fig. 2(a), a diagram is shown for the values of argument of the complex variable A_1 recorded stroboscopically at $t = t_n = (n + \frac{9}{20})T$. Indeed, the plot demonstrates the doubling of the
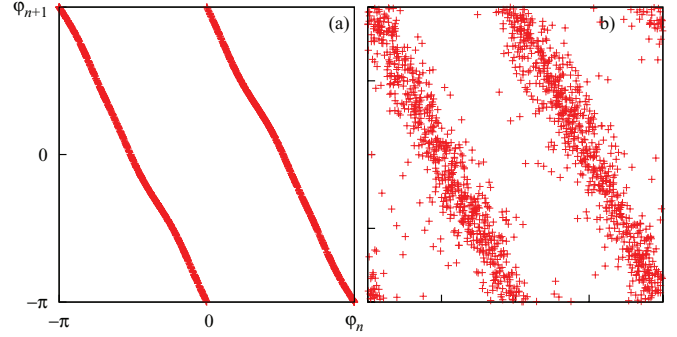

FIG. 2. (Color online) (a) The plot φ_{n+1} vs. φ_n where $\varphi_n = \arg A_1(nT + \frac{9}{20}T)$, and A_ℓ is a solution of Eqs. (12). (b) The same diagram for the ensemble Eq. (14), where A_1 is computed according to Eq. (3). Parameters are the same as those described in the legend of Fig. 1.

phase, as expected. Thus, actually, the phases of the alternately arising clusters evolve according to the expanding circle map that implies hyperbolic chaos.

B. Ensemble of noisy oscillators

Here we report on the results of a straightforward simulation of the ensemble dynamics according to Eqs. (14). We perform numerical solutions for these stochastic differential equations employing a special version of the Runge-Kutta-type algorithm suggested in Ref. [26]. Figure 1(d) illustrates temporal behavior of the probability density $v(\phi,t)$ computed from the instantaneous distributions of the phases ϕ_k for the elements of the ensemble, and Figs. 1(e) and 1(f) demonstrate the dynamics of the mean-field variables $A_n(t)$. The parameters are the same as in the previous simulations of the Fokker-Plank equation. Except for the obvious difference in the initial conditions, the distributions $v(\phi,t)$ and the magnitudes of $A_n(t)$ at their high levels behave visually similar. The dynamics of the phases is definitely more noisy than that in Fig. 1(c), especially in the regions where the magnitudes of the corresponding modes are small: in these regions, even small finite-size fluctuations produce a large effect on the phases. When the magnitude of $A_1(t)$ is high (see for example the time interval $30 < t < 75$), its argument does not respond to the noise. But when A_1 gets small, the argument fluctuates (see the time interval $110 < t < 150$). The same is true for A_2. The most harmful are the fluctuations of Φ_1, because this variable inherits the argument value from A_2 when $|A_1|$ is small. If the fluctuations are strong enough, they wash out the correct value of the argument, and the phase multiplication mechanism ceases to operate properly. The fluctuations of A_2 are not so essential since they occur only in epochs, when the component A_2 does not play an important role. One can see from Fig. 1 that the phase transfer happens when A_2 has a large magnitude and thus is not affected by the noise (see the time interval $180 < t < 225$).

Figure 2(b) shows the diagram for the stroboscopically recorded values of Φ_1 corresponding to the dynamical behavior illustrated in Figs. 1(d)–1(f). One can observe that the phases demonstrate the expected Bernoulli-like doubling mapping in average, though the fluctuations produce a noticeable
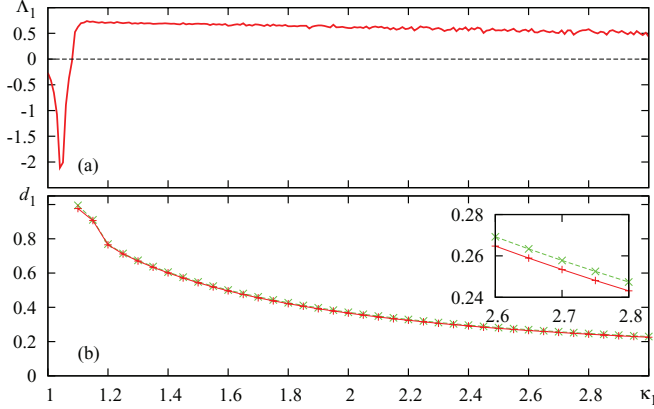
FIG. 3. (Color online) (a) The first Lyapunov exponent and (b) the lower and upper boundaries of the distribution of d_1 vs. κ_1. The data relate to the stroboscopic map corresponding to the Fokker-Plank system Eq. (12) at $t_n = (n + \frac{9}{20})T$. Distributions of d_1 for each κ_1 were computed for 10^4 attractor points. $\kappa_2 = 2.3$; other parameters are the same as described in the legend of Fig. 1.

FIG. 4. (Color online) The same quantities as described in the legend of Fig. 3 against κ_2, while $\kappa_1 = 1.3$.

statistical widening (which decreases as the size of the ensemble K grows).

C. Lyapunov exponent and hyperbolicity test

Now we return to the Fokker-Plank system Eq. (12) and discuss how the Lyapunov exponents (LEs) depend on κ_1 and κ_2. Also, we test hyperbolicity of the chaotic dynamics of the system Eq. (12).

We calculate the Lyapunov exponents in the deterministic system Eq. (12) with the standard algorithm due to Benettin *et al*. Because the system is periodically driven, we report as LEs the values $\Lambda = \lambda T$, i.e., the "Lyapunov multipliers" over the period. In all cases we have found at most one positive LE, the others were negative. Figure 3(a) shows the largest LE versus parameter κ_1; in a large range of this parameter it is positive and close to the expected value $\ln 2 \approx 0.69314$. The other exponents are all negative, and their magnitudes are much higher. For example, at $\kappa_1 = 1.3$ and $\kappa_2 = 2.3$ we have $\Lambda_i = \{0.688, -17.355, -197.507, -245.781, -705.748\}$, and the corresponding Kaplan-Yorke dimension is 1.04.

The positive Lyapunov exponent varies slowly depending on the parameter, but no tips or dips, like in many nonhyperbolic systems, are observed. This may be regarded as a manifestation of the structural stability intrinsic to the hyperbolic dynamics. Figure 4(a) represents a dependence of Λ on κ_2, while κ_1 is constant. Again, the same features are observed: the largest Lyapunov exponent is close to the value $\ln 2$, and it does not demonstrate any notable variation within a wide range of the parameter.

To test hyperbolicity, we employed the method that has been specially developed for high-dimensional systems; see Ref. [27] for the details and Ref. [28] for the mathematical background. In brief, the method includes the computation of the first k orthogonalized Lyapunov vectors moving forward in time (so called Gram-Schmidt vectors or backward Lyapunov vectors [28]), and also the first k orthogonalized Lyapunov vectors obtained moving backward in time from the conjugate
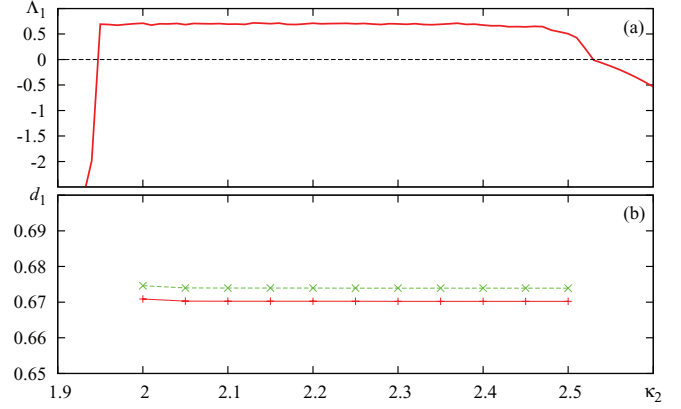
variational equations (forward Lyapunov vectors); here k is the dimension of the unstable manifold. Given these vectors, a $k \times k$ matrix of their scalar products is built. Its smallest singular value d_k is cosine of the angle between the expanding tangent subspace and the orthogonal complement to the contracting tangent subspace, and thus d_k can be used as an indicator of hyperbolicity. For a nonhyperbolic case, the d_k values vanish somewhere along trajectories (as tangencies between the associated expanding and contracting subspaces occur), but for situations of hyperbolic dynamics the distribution of d_k is well separated from zero.

In Fig. 3(b) we illustrate the results of this hyperbolicity test. In our case the expanding subspace is one-dimensional. Thus, for each κ_1 we compute 10^4 points on the attractor of the stroboscopic map and evaluate the indicator d_1 at each of them. Then, the smallest and the largest values of d_1 are plotted on the diagram, marked with crosses and pluses, respectively. The first observation is that the smallest d_1 is very well separated from zero; this confirms the hyperbolicity. Another noteworthy observation is that the maximal and the minimal values of d_1 are very close to each other. This means that the mutual orientations of the expanding and contracting directions remain practically unaltered on the entire attractor. This can be treated as another manifestation of the structural stability. Figure 4(b) shows the hyperbolicity indicator d_1 in dependence on κ_2, it is again well separated from zero.

D. Lyapunov exponents for the microlevel dynamics

It is instructive to compare the macroscopic LEs for the dynamics of the order parameters with microscopic LEs describing stability of the dynamics of individual oscillators. A direct approach to computation of the full spectrum of Lyapunov exponents for the ensemble of phase oscillators Eq. (14) can easily exhaust a computer memory and take an extremely long time. However, there is a simple way to estimate microscopic LEs assuming their decoupling from the macroscopic dynamics. Neglecting small ϵ in Eq. (3), we can rewrite this equation as

$$\dot{\phi}_k = \frac{1}{2i} \sum_{n=1}^{2} \tilde{\kappa}_n (A_n e^{-in\phi_k} - A_n^* e^{in\phi_k}) + \sigma \xi_k(t). \quad (15)$$

Let us now assume that on stages 1 and 2, the order parameters A_1 and A_2 are roughly constant. Then the variations of the phases satisfy

$$\frac{1}{\delta\phi_k}\frac{d}{dt}\delta\phi_k = -\sum_{n=1}^{2} n\tilde{\kappa}_n(A_n e^{-in\phi_k} + A_n^* e^{in\phi_k}). \quad (16)$$

Now the microscopic LE is evaluated as an average of the right-hand side of Eq. (16) multiplied by $T/2$, which yields $\Lambda_{\mathrm{mic}} = -\frac{T}{2}\sum_{n=1}^{2} n\tilde{\kappa}_n|A_n|^2$. Substituting here the approximate expressions for stationary magnitudes of the order parameters, valid for small subcritical couplings $\kappa_1 \gtrsim \sigma^2$, $\kappa_2 \gtrsim 2\sigma^2$, we obtain the following estimate:

$$\Lambda_{\mathrm{mic}} \approx -T\sigma^2\left(\frac{\kappa_1 - \sigma^2}{\kappa_1} + 4\frac{\kappa_2 - 2\sigma^2}{\kappa_2}\right). \quad (17)$$

For the parameters used above, $\sigma = 1, \kappa_1 = 1.3, \kappa_2 = 2.3, T = 150$, this yields $\Lambda_{\mathrm{mic}} \approx -113$ in a reasonable agreement with the numerics.

Thus, contrary to many situations where chaos occurs in the microlevel description, while the macroparameters manifest rather regular behavior, here we observe an impressive opposite case: the microdynamics is stable (because $\Lambda_{\mathrm{mic}} < 0$), but at the macrolevel, hyperbolic chaos takes place.

V. CONCLUSION

In this paper we have demonstrated that blinking coupling in populations of noisy oscillators may result in hyperbolic chaos of macroscopic mean fields. The blinking is between two simplest modes of coupling: one leads to a one-cluster synchronized state, another one leads to appearance of two clusters, shifted by π. Correspondingly, at these couplings two different order parameters dominate: the usual Kuramoto order parameter for the one-cluster state, and the second-harmonics Daido order parameter for the two-cluster state. While the magnitudes of these order parameters show no significant variations from cycle to cycle, the phases obey a strongly chaotic Bernoulli transformation and thus demonstrate hyperbolic chaos. Noteworthy, there is a realistic situation where the two types of global coupling (one-cluster and two-cluster) can be

observed: this is an ensemble of pendula hanging on a common beam. In such a configuration with two pendulum clocks, Ch. Hyugens observed synchronization more than 300 years ago (see a translation of his notes in Ref. [2]). Nowadays one reproduces these experiments with metronomes [29]. The horizontal motions of the beam result in the one-cluster coupling, while the vertical motions lead to the two-cluster coupling [30].

Our analysis is mostly based on the consideration of the thermodynamic limit, where the population can be described by the nonlinear Fokker-Planck equation. We verify hyperbolic chaos in this integral-differential equation, by direct simulations of equations for the modes and showing that their phases obey a Bernoulli map and by checking that the stable and the unstable directions in the tangent space are never tangent to each other. For the original population, a direct simulation gives a picture very similar to that for the nonlinear Fokker-Planck equation, but the one-dimensional transformation of the phases looks like a noisy Bernoulli map, due to finite-size effects.

In a more general perspective, the nonlinear Fokker-Planck equation, as an integrodifferential equation with partial derivatives, is a representative of a class of deterministic distributed systems demonstrating pattern formation. Different cluster synchronization states correspond to different patterns; phases of clusters correspond to the spatial positions of the patterns. With this interpretation, our results demonstrate that an interaction between blinking patterns results in a chaotic relocation of their positions; moreover, this chaos is hyperbolic. A kind of such behavior was reported recently in a model of interacting Turing patterns with different wave numbers [24]. The presented model based on the nonlinear Fokker-Planck equation provides another indication that the above mechanism of the hyperbolic chaos is realizable in quite generic circumstances.

[1] Y. Kuramoto, *Chemical Oscillations, Waves and Turbulence* (Springer, Berlin, 1984) .

[2] A. Pikovsky, M. Rosenblum, and J. Kurths, *Synchronization. A Universal Concept in Nonlinear Sciences* (Cambridge University Press, Cambridge, 2001) .

[3] E. Ott and Th. M. Antonsen, Chaos **18**, 037113 (2008).

[4] K. Kaneko, Physica D **55**, 368 (1992).

[5] A. S. Pikovsky and J. Kurths, Physica D **76**, 411 (1994).

[6] A. Pikovsky, M. Rosenblum, and J. Kurths, Europhys. Lett. **34**, 165 (1996).

[7] D. Topaj, W.-H. Kye, and A. Pikovsky, Phys. Rev. Lett. **87**, 074101 (2001).

[8] E. Ott, P. So, E. Barreto, and T. Antonsen, Physica D **173**, 29 (2002).

[9] V. Hakim and W. J. Rappel, Phys. Rev. A **46**, R7347 (1992).

[10] N. Nakagawa and Y. Kuramoto, Physica D **75**, 74 (1994).

[11] S. P. Kuznetsov, A. Pikovsky, and M. Rosenblum, Chaos **20** (2010).

[12] R. C. Desai and R. Zwanzig, J. Stat. Phys. **19**, 1 (1978).

[13] D. A. Dawson, J. Stat. Phys. **31**, 29 (1983).

[14] L. L. Bonilla, J. C. Neu, and R. Spigler, J. Stat. Phys. **67**, 313 (1992).

[15] A. Pikovsky and S. Ruffo, Phys. Rev. E **59**, 1633 (1999).

[16] Igor V. Belykh, Vladimir N. Belykh, and Martin Hasler, Physica D: Nonlinear Phenomena **195**, 188 (2004).

[17] Lei Wang, Huan Shi, and You-xian Sun, Phys. Rev. E **82**, 046222 (2010).

[18] Maurizio Porfiri, Phys. Rev. E **85**, 056114 (2012).

[19] S. P. Kuznetsov, *Hyperbolic Chaos: A Physicist's View* (Higher Education Press, Bejing, and Springer-Verlag, Berlin/Heidelberg, 2012), p. 336.

[20] S. P. Kuznetsov, Phys. Usp. **54**, 119 (2011).

[21] S. Smale, Bull. Am. Math. Soc. **73**, 747 (1967).
[22] S. P. Kuznetsov, Phys. Rev. Lett. **95**, 144101 (2005).
[23] S. P. Kuznetsov and A. Pikovsky, Physica D **232**, 87 (2007).
[24] P. V. Kuptsov, S. P. Kuznetsov, and A. Pikovsky, Phys. Rev. Lett. **108**, 194101 (2012).
[25] S. M. Cox and P. C. Matthews, J. Comput. Phys. **176**, 430 (2002).
[26] R. L. Honeycutt, Phys. Rev. A **45**, 600 (1992).

[27] P. V. Kuptsov, Phys. Rev. E **85**, 015203 (2012).
[28] P. Kuptsov and U. Parlitz, J. Nonlinear Sci. **22**, 727 (2012).
[29] M. Kapitaniak, K. Czolczyński, P. Perlikowski, A. Stefański, and T. Kapitaniak, Phys. Rep. **517**, 1 (2012).
[30] K. Czolczyński, P. Perlikowski, A. Stefański, and T. Kapitaniak, Commun. Nonlinear Sci. Numer. Sim. **18**, 386 (2013).